Determination of the Azimuthal Asymmetry in Deuteron Disintegration by Linearly Polarized Photons at $E_\gamma = 1.1 - 2.3$ GeV

R. Avakian[1], L. N. Ananikyan, N. Ya. Ivanov[1,2], S. Taroyan
Yerevan Physics Institute, Alikhanian Br.2, 375036 Yerevan, Armenia

B. L. Berman[1], Y. Y. Ilieva, and P. Nadel-Turonski
The George Washington University, Washington, DC, 20052

M. Mirazita and P. Rossi
Laboratori Nazionali di Frascati, INFN, 00044 Frascati, Italy

K. Livingston
University of Glasgow, Glasgow G12 8QQ, United Kingdom

G. P. Gilfoyle
University of Richmond, Richmond, Virginia 23173

H. Avakian and V. D. Burkert
Thomas Jefferson National Accelerator Facility, Newport News, Virginia 23606

Abstract

We propose to determine the azimuthal asymmetry in deuteron disintegration by linearly polarized photons in the energy range $E_\gamma = 1.1 - 2.3$ GeV using the CLAS data gathered in the g13 experiment. The aim of this work is to search for quark and gluon degrees of freedom in the nuclear state. The measurement of the beam-spin asymmetry in deuteron photodisintegration will provide: *a*) novel spin-dependent information on the underlying mechanism complementary to the production cross section and recoil-proton polarizations; *b*) improvement of our understanding of the role and region of applicability of perturbative QCD at low and intermediate energies; *c*) stringent constraints on the nonperturbative QCD-based models of photonuclear reactions.

1 Physics Motivation

1.1 *Scaling laws in QCD and experimental data*

The process of deuteron photodisintegration,

$$\gamma + d \to n + p, \tag{1}$$

is especially important for the investigation of the role of quarks and gluons in nuclear interactions. This photonuclear reaction is: *i)* simplest ($A = 2$) and *ii)* well studied experimentally. During the last 15 years, a number of experiments have been performed for measuring its differential cross section over a

[1]Co-spokesperson
[2]Contact person

broad range in energy and angle [1, 2, 3, 4, 5, 6, 7, 8]. There are also some data on the recoil proton polarization [9, 10] and the single beam-spin asymmetry [11, 12].

The most remarkable property of the available data is the energy behavior of this photonuclear process. At $E_\gamma \geq 1$ GeV and large scattering angles, it was found that $\mathrm{d}\sigma/\mathrm{d}t(s, \theta_{cm}) \sim s^{-11}$, where s and t are the usual Mandelstam variables, while θ_{cm} is the scattering angle in the center-of-mass frame (for more details, see Ref. [13]). Just such a behavior is predicted by the constituent counting rules (CCR) based on the scaling law for the hadron wave functions [14, 15]. For an arbitrary exclusive two-body reaction, CCR predict a power-law falloff of the production cross section at fixed angles:

$$\mathrm{d}\sigma/\mathrm{d}t \sim h(\theta_{cm})/s^{n-2}, \tag{2}$$

where n is the total number of elementary fields in the initial and final states, while $h(\theta_{cm})$ depends on details of the dynamics of the process.

The quark counting rule was originally obtained based on dimensional analysis under the assumptions that the only scales in the system are momenta and that composite hadrons can be replaced by point-like constituents [14, 15]. Contributions from the quark orbital angular momentum have also been neglected. Later, these counting rules were confirmed within the framework of perturbative QCD (pQCD) analysis up to logarithmic factors [16]. This analysis relies on the factorization of the exclusive process into a hard-scattering amplitude and a soft-quark amplitude inside the hadron. Finally, in the last few years, an all-orders demonstration of the counting rules for hard exclusive processes has been shown to arise from the correspondence between the string theory in anti-de Sitter space and conformal field theories (AdS/CFT) in physical space-time [17]. The AdS/CFT correspondence [18] leads to an analytical, semi-classical model for strongly-coupled QCD which has scale invariance and dimensional counting at short distances and color confinement at large distances.

An approximate dimensional scaling has been observed in many exclusive reactions at sufficiently high energy and large momentum transfer (for reviews see Refs. [19, 20]). Surprisingly, the low-energy data on deuteron disintegration [1, 2, 3, 4, 5, 6, 7, 8] (as well as the charged-pion photoproduction [21]) also demonstrate a similar trend (*i.e.*, scaling behavior). In fact, dimensional scaling can be justified only in the high-energy limit, $t \sim s \gg m^2$, when one can neglect all the masses of the interacting particles. Therefore, it seems naive to expect that the CCR will hold in the few-GeV region. A natural question then arises: what mechanism is really responsible for the observed energy behavior of the reaction (1)?

Towards this goal, it is useful to look closely at claims of agreement between the data for differential cross sections and the CCR predictions. Historically, elastic proton-proton (pp) scattering at high energy and large momentum transfer has played a very important role in the development of QCD. In fact, the re-scaled 90° center-of-mass pp elastic scattering data, $s^{10}\mathrm{d}\sigma/\mathrm{d}t$, show substantial oscillations about the power-law behavior [22, 23]. Such oscillations are also seen in πp fixed-angle scattering [24]. The old data [19] as well as the new data from JLab experiment E94-104 on photoproduction of charged pions at $\theta_{cm} = 90°$ [21] also show hints of oscillation about the expected s^{-7} scaling. There are hints of scaling behavior in $\gamma d \to d\pi^0$ as well [25, 26] (s^{-13} in this case). In addition to violation of the scaling laws, spin correlations in polarized pp elastic scattering [27, 28] also show significant deviations from naive perturbative QCD expectations (the so-called hadron helicity conservation, HHC, rules).

Theoretical interpretation of this oscillatory behavior of the scaled cross section ($s^{10}\mathrm{d}\sigma/\mathrm{d}t$) in pp scattering was attempted by many authors. Some explained this feature in terms of the opening up of a $c\bar{c}uuduud$ resonant state [29]; others as the result of the interference between the short-distance (pQCD)

and long-distance (Landshoff) amplitudes [30, 31]. As shown in [32, 33], gluonic radiative corrections to the long-distance amplitude give rise to a nontrivial phase and thus an energy-dependent oscillation. In Ref. [34], a similar interference concept has been applied to describe the *pp* polarization data.

Very recently, a number of new developments have generated renewed interest in this topic. Zhao and Close [35] have argued that a breakdown in the locality of quark-hadron duality (called "restricted locality") results in oscillations around the scaling curves predicted by the counting rule. They explain that, at high energies, the smooth behavior of exclusive cross sections according to the scaling laws arises from destructive interference between various intermediate-resonance states. However, at lower energies this cancellation due to destructive interference breaks down locally and gives rise to oscillations about the smooth behavior.

On the other hand, Ji, Ma, and Yuan [36] have derived a generalized counting rule based on pQCD analysis. Their generalized counting rule for hard exclusive processes includes parton orbital angular momentum and hadron helicity flip; thus they provide the scaling behavior of the helicity-flipping amplitudes. The interference between the different helicity flip and non-flip amplitudes offers a new mechanism to explain the oscillations in the scaling cross sections and spin correlations. Dutta and Gao [37] have used this approach to describe successfully the polarized elastic *pp* scattering data.

Brodsky and de Teramond [38] used AdS/CFT duality to include the orbital angular momentum of the constituents in hadronic light-front wave functions. This yields an equivalent (to perturbative QCD) dimensional counting rule for the hadron form factors, but here the analysis is performed in the strong coupling regime without the use of perturbation theory. Like the pQCD results [39], the light-front calculations [40] based on the AdS/CFT correspondence explain well the proton form-factor ratio $G_E(Q^2)/G_M(Q^2)$ measured recently at JLab in polarization-transfer experiments [41].

In conclusion, we see that experimental investigations of the scaling phenomena and related spin-dependent effects have stimulated significant theoretical advances in understanding of the role and range of applicability of perturbative QCD at low and intermediate energies. These studies make it possible to develop in detail a number of nonperturbative QCD-based approaches to the hadronic dynamics at long distances. The results achieved to the date provide a strong motivation for further investigation of scaling laws and spin effects in photonuclear reactions as well. Proposed measurement of the azimuthal beam-spin asymmetry in deuteron photodisintegration can give access to important aspects of the underlying physics, such as QCD final-state interactions and quark orbital angular momentum in the lightest nuclei.

1.2 *Theoretical models and experimental status of deuteron photodisintegration*

At low energies, the nuclear dynamics is usually described in terms of nucleonic degrees of freedom. There have been many attempts to understand low-energy deuteron photodisintegration using a conventional meson-baryon framework (for a review see Ref. [42]). Within the context of QCD, this hadronic picture is expected to break down at sufficiently high energies where the basic degrees of freedom must be quarks and gluons. The most popular quark-gluon models for deuteron photodisintegration are the reduced nuclear amplitudes (RNA) model [43, 44], the hard-rescattering mechanism (HRM) [45, 46], and the quark-gluon string model (QGSM) [47, 48].

To extend the region of applicability of pQCD down to lower momentum transfers, Brodsky and Hiller introduced the idea of reduced nuclear amplitudes [43]. In this model, the gluon exchanges that contribute to identifiable subprocesses (such as nucleon form factors) are collected together and their contributions

replaced by experimentally determined nucleon form factors. It is hoped that the resulting expressions will correctly include much of the missing soft physics, and will therefore be valid to lower momentum transfers than the original pQCD expressions from which they were obtained.

In the HRM [45, 46], the quark exchange mechanism is explored. The matrix element is written as a convolution of an elementary quark exchange interaction with the initial and final nucleon wave functions. The final nucleons are free and the distribution of initial nucleons is given by the deuteron wave function. Since the photon momentum is shared by the proton and neutron, there is little sensitivity to the high momentum part of the deuteron wave function. The elementary interaction is a quark exchange between the two nucleons, with the photon absorbed by one quark which then gives up its momentum through a hard gluon exchange with another quark. Frankfurt, Miller, Sargsian and Strikman show that this can be replaced approximately by the wide angle *pn* scattering cross section, also dominated by quark exchange. The authors propose using experimental data for the *pn* cross sections. However, since data do not exist for the actual kinematic conditions needed, it must be extrapolated and predictions for photodisintegration are given as a band corresponding to the uncertainties introduced by the interpolation. Originally, the authors believed that their predictions should be valid for $E_\gamma > 2.5$ GeV and nucleon momentum transfers $-t$, $-u > 2$ GeV^2. Then they used the model at lower energies, down to $E_\gamma = 1$ GeV.

Another approach to the problem of long-distance dynamics is used in the QGSM proposed by Kaidalov in Refs. [49]. This model is based on two ingredients: *i)* a topological expansion in QCD and *ii)* a space-time picture of interactions between hadrons that takes into account the confinement of quarks. In a general sense, the QGSM can be considered as a microscopic (nonperturbative) model of Regge phenomenology for the analysis of exclusive and inclusive hadron-hadron and photon-hadron reactions at the quark level. In Refs. [47, 48], this approach has been applied to the analysis of the angular and energy dependence of the differential cross section for the reaction $\gamma d \to np$ in the few-GeV region. Originally, the QGSM was formulated for the case of small scattering angles (*i.e.*, low momentum transfers). Later, Kondratyuk *et al.* extrapolated the QGSM amplitudes to the case of large-angle deuteron photodisintegration [48]. Following Refs. [50], they assumed that there is only a single Regge term that connects smoothly the low and high momentum transfer regions. These authors require that the matrix element at fixed angle be obtained either as a large-t limit of the forward Regge form or as a large-u limit of the backward scattering amplitude. To obey this condition, a logarithmic parametrization for the nucleon trajectory was adopted.

Figure 1 shows the results (both theoretical and experimental) for the differential cross section $\mathrm{d}\sigma/\mathrm{d}t$ multiplied by the factor s^{11} predicted by CCR and plotted as a function of E_γ for four regions of the proton scattering angle.[3] All of the available high-energy data ($E_\gamma \gtrsim 1$ GeV) are presented here. We see that the cross-section data for $60^\circ \leq \theta_{cm} \leq 90^\circ$ are in agreement with the CCR expectations. The cross sections at the forward angles fall off more slowly.

The HRM [45, 46] (hatched band) agrees reasonably well with the existing data up to about 4 GeV, then tends to be higher at forward angles. The RNA calculation (dashed line) is only available at $\theta_{cm} = 90^\circ$ [51]. The predictions of the asymptotic meson exchange current (AMEC) model [52] are given by dotted lines. This approach is formulated in terms of nucleonic and mesonic degrees of freedom and predicts a slightly different energy dependence. In particular, the AMEC model overestimates the data at energies between 1.6 and 2.0 GeV. The QGSM describes well the data at all four proton angles. The largest

[3] Figures 1 and 2 are taken from Refs. [8] and [10], respectively.

discrepancy is found at 30°-40° above 3 GeV where it suggests a slower decrease of the cross section with energy than is observed.

Summarizing the results on the production cross sections, one can conclude that the approaches based on various physical principles describe, with about the same degree of success, the available data on the angular and energy dependence of the reaction. Thus, for a better understanding of the underlying mechanism, complementary information on the spin-dependent observables is necessary.

Concerning the polarization observables, there are only three sets of data for deuteron photodisintegration at energies above 1 GeV. The azimuthal beam-spin asymmetry Σ was measured at Yerevan [11, 12]; the induced proton polarization p_y and the polarization transfers $C_{x'}$ and $C_{z'}$ were measured at JLab [11, 12]. On the theoretical side, two calculations of the spin observables are available, within the QGSM [53] and HRM [54] frameworks.

The data on the recoil proton polarization parameters obtained in two recent JLab experiments at $E_\gamma \approx 2$ GeV are presented in Fig. 2. We see that the QGSM [53] predicts the longitudinal polarization transfer $C_{z'}$ in good qualitative agreement with the measured data, but makes no prediction for the transverse polarizations p_y and $C_{x'}$ due to their sensitivity to the relative phase of the helicity amplitudes.

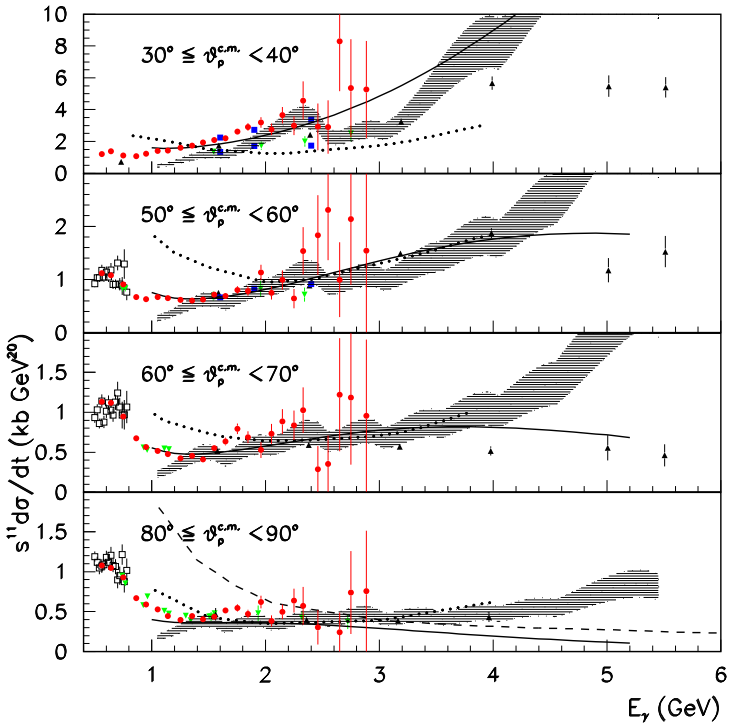

Figure 1: Deuteron photodisintegration cross sections $s^{11}d\sigma/dt$ as a function of E_γ for the proton scattering angles noted. Results from CLAS [8] (full/red circles), Mainz [4] (open squares), SLAC [1, 2, 3] (full/green down-triangles), JLab Hall A [7] (full/blue squares) and Hall C [5, 6] (full/black up-triangles) are included, as well as predictions of the QGSM [48] (solid line), AMEC [52] and RNA [43] models (dotted and dashed lines, respectively), and the HRM [45] model (hatched area).

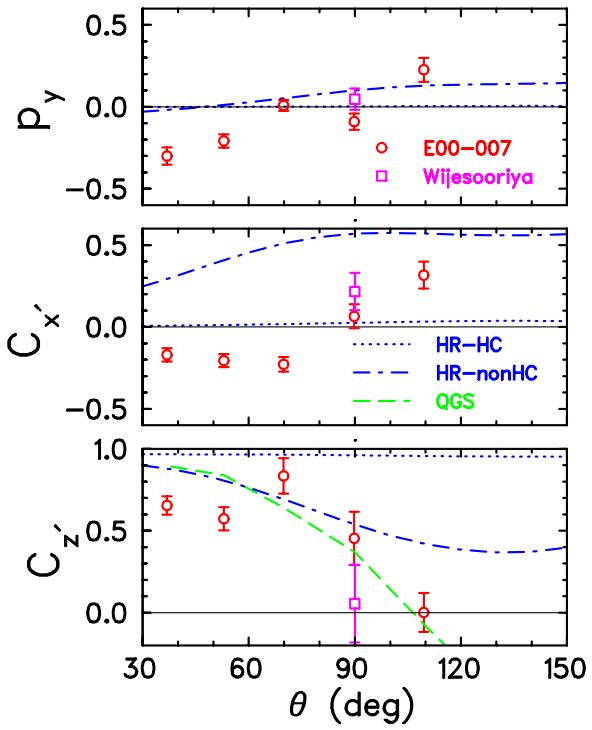

Figure 2: Polarization transfers $C_{x'}$, $C_{z'}$ and induced polarization p_y in deuteron photodisintegration.

In this respect, calculations of $C_{z'}$ are more stable because they do not depend on this phase but only on the moduli squared of the helicity amplitudes.

Figure 2 also shows predictions for all three observables from the HRM [54]. It should be noted that these calculations are at the lower edge of the nominal validity range of the model. Also, since the pn spin amplitudes are not well constrained by data, the pn amplitudes are based on pp data. Thus, there are large uncertainties in the predictions. One calculation (dotted line) assumes that there is only small helicity nonconservation, leading to small values of $C_{x'}$ and p_y, and $C_{z'}$ being nearly unity. The second (dash-dot line) calculation assumes large helicity non-conservation. The comparison with all observables supports large helicity nonconservation, but clearly the predictions for the transverse polarization do not agree with the data. Thus, the two models, QGSM and HRM, which predict the longitudinal polarization transfer are in qualitative agreement with available data, while neither model adequately explains the transverse polarizations.

The situation is completely unclear for the case of the azimuthal beam-spin asymmetry Σ, defined as

$$\Sigma = \frac{1}{\mathcal{P}_\gamma} \frac{N_\parallel - N_\perp}{N_\parallel + N_\perp}, \tag{3}$$

where $\mathcal{P}_\gamma$ is the degree of linear polarization of the incident photon beam and $N_\parallel$ and $N_\perp$ are the numbers of events produced in the parallel and perpendicular (relative to the photon polarization) directions, respectively. For the asymmetry Σ, there are only Yerevan data in the energy range 0.8-1.6 GeV and at $\theta_{cm} = 90^\circ$ [11, 12]. Unfortunately, the data at $E_\gamma \approx 1.4$-1.6 GeV have large uncertainties, which do not allow us to test the models under consideration. However, the Yerevan data indicate that $\Sigma(90^\circ)$ might

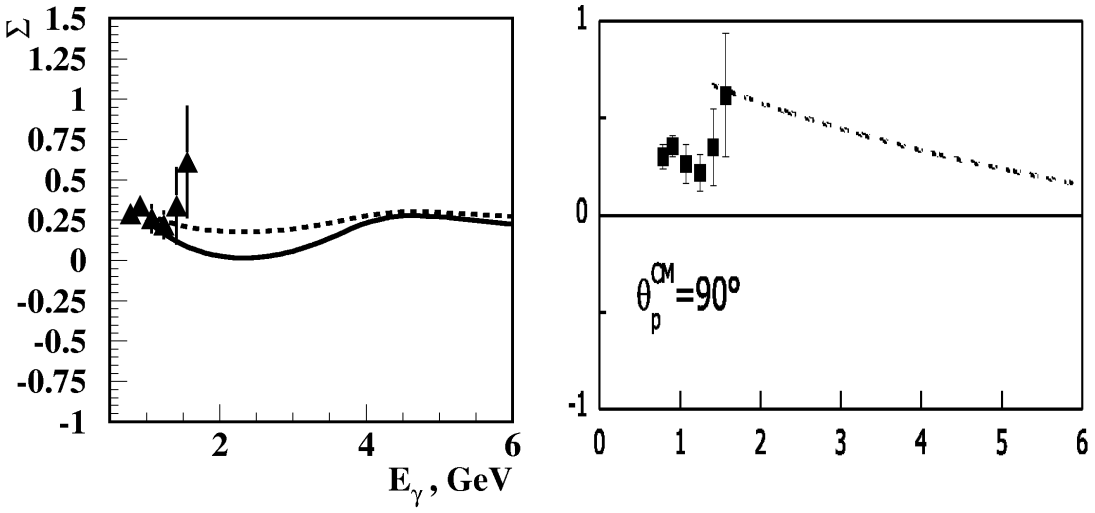

Figure 3: The HRM (*left panel*) and QGSM (*right panel*) predictions for the single beam-spin asymmetry Σ at $\theta_{cm} = 90^\circ$. The figures are taken from the Refs. [54] and [53], respectively.

be large (about 50%) at these energies. This fact could be crucial for the determination of the mechanism mainly responsible for deuteron photodisintegration. In fact, the QGSM is able to accommodate a large ($\sim 50\%$) azimuthal asymmetry at $E_\gamma \approx 1.6$ GeV and $\theta_{cm} = 90^\circ$ [53], while the HRM is not able to do so [54].

Theoretical predictions and available data [11, 12] for the asymmetry Σ at $\theta_{cm} = 90^\circ$ are shown in Fig. 3. The left panel shows the HRM results [54]. Again, the solid and dashed curves correspond to two different, "on-shell" and "off-shell", parametrizations of the helicity flip amplitude. In both cases, the asymmetry $\Sigma(90^\circ)$ is predicted to be less than 25% in the entire photon-energy range. The QGSM calculations [53] are presented in the right panel of Fig. 3. We see that the model predicts a large ($\sim 50\%$) value for $\Sigma(90^\circ)$ at $1.5 \lesssim E_\gamma \lesssim 2.0$ GeV.

Summarizing, measurements of the azimuthal beam-spin asymmetry Σ for deuteron photodisintegration will give important complementary information on the underlying mechanism, and could thus provide a crucial test of nonperturbative calculations.

2 Our Proposed Work

The Proposal We propose to determine the azimuthal asymmetry Σ for deuteron disintegration by linearly polarized photons for E_γ =1.1-2.3 GeV using the CLAS data gathered in the g13 experiment on kaon photoproduction [55]. The asymmetry $\Sigma(s,t)$ is related to the doubly-differential cross section for the reaction (1)

$$\frac{\mathrm{d}^2\sigma}{\mathrm{d}t\mathrm{d}\varphi}(s,t,\varphi) = \frac{1}{2\pi}\frac{\mathrm{d}\sigma_{unp}}{\mathrm{d}t}(s,t)\left[1 + \mathcal{P}_\gamma \Sigma(s,t)\cos 2\varphi\right], \tag{4}$$

where $\mathrm{d}\sigma_{unp}/\mathrm{d}t$ is the unpolarized $\gamma d \to pn$ cross section and φ is the azimuthal angle between the beam polarization direction and the observed nucleon transverse momentum p_T.

It would be very useful (from both theoretical and experimental points of view) to have the asymmetry data obtained under the same conditions and in the same angular and energy range as the results on the

deuteron photodisintegration cross section reported recently by the CLAS collaboration [8]. By combining our anticipated data for Σ with the existing results for $d\sigma/dt$ [8] and recoil proton polarizations (p_y, $C_{x'}$,$C_{z'}$) [9], we will obtain a practically complete experimental description of deuteron photodisintegration in the 1-2 GeV energy region that will provide a stringent constraint on the theory.

Experimental Setup In the CLAS g13 experiment, data were obtained for six photon-energy bins in the range 1.1-2.3 GeV, in steps of 200 MeV. The linear polarization of the photons is practically constant over each 200-MeV region. The mean value of the beam polarization varies slowly from $\mathcal{P}_\gamma \approx 90\%$ at $E_\gamma = 1.2$ GeV to $\mathcal{P}_\gamma \approx 70\%$ at $E_\gamma = 2.2$ GeV [55, 56].

In our proposed analysis, the photodisintegration events will be identified by two different (independent) methods. The first one is to select the events with a single charged particle (proton) in the final state and to apply a missing-mass cut to the reaction $\gamma d \to pX$. In the second case, we shall use the exclusive events where both the proton and the neutron are detected, the latter in the electromagnetic calorimeter. The reconstruction efficiency of relatively high energy neutrons at large angles, required for our proposed studies, is estimated to be $\sim$ 35-40% [57]. The convergence of both methods at small angles would be an excellent test of our analysis.

Due to the complexity of the CLAS detector, it is crucial to make sure that the momentum determined by the drift-chamber tracking system is reliable. For this reason, the position of the peak of the missing-mass distributions for $\gamma d \to pX$ events should be checked over the whole range of proton momenta and scattering angles. To obtain the correct position of the peak in each kinematic bin, we must take into account the proton energy loss in the target and detector with the help of a corresponding correction function [59]. The background contribution to the number of total events under the peak can be evaluated by integrating an appropriate exponential fit function between the missing mass cuts [8].

The efficiency of single-proton detection in CLAS was analyzed in Ref. [8] as a function of azimuthal angle φ. It was found that this function is constant in the central azimuthal regions of the six CLAS sectors and decreases steeply near the sector boundaries. For this reason, only events in the central regions with uniform efficiency of the detector will be used.

Statistical Uncertainties Our estimates of the number of the expected photodisintegration events N in a specific kinematic bin $(E_\gamma, \cos\theta_{cm})$ are based on the preliminary analysis of the g13 results (see Section 4) as well as on the data [8] for $d\sigma/dt$. Having the total number of unpolarized events N, one can calculate the statistical uncertainty $\delta\Sigma = \frac{1}{\mathcal{P}_\gamma}\frac{1}{\sqrt{N}}$. In particular, at $\theta_{cm} = 90^\circ$ the expected statistical error is $\delta\Sigma(90^\circ) = (1.8, 1.9, 3.2, 3.8, 5.8, 8.6)$ % for the photon-energy bins centered at $E_\gamma = (1.2, 1.4, 1.6, 1.8, 2.0, 2.2)$ GeV. At smaller angles the uncertainties decrease because of the higher counting rate. Thus it will be possible to measure the asymmetry Σ with a precision of a few percent.

Systematic Uncertainties For the unpolarized case, the systematic uncertainties come from the total number of incident photons, the target length and density, the proton detection efficiency, and the background contributions. The resulting total systematic uncertainty for the disintegration cross section is less than 10% for all the kinematic bins $(E_\gamma, \cos\theta_{cm})$ under consideration [8]. However, for the case of the beam-spin asymmetry Σ, the corresponding uncertainty should be significantly smaller because most of the above uncertainties cancel out in the ratio (3).

Uncertainties in the linear polarization of the photon beam have been investigated for a JLab experiment [56]. A value of 5% was found for the relative uncertainty $\delta\mathcal{P}_\gamma/\mathcal{P}_\gamma$ that should be taken into account in the determination of the systematic uncertainty.

In principle, incomplete azimuthal acceptance of the CLAS equipment can produce errors in measurements of the beam-spin asymmetries. To avoid this problem, half of the statistics in the g13 experiment was collected with the photon beam polarization rotated by 90°. This should lead to the cancellation of any false asymmetries. Therefore, we do not anticipate any uncertainty due to the CLAS φ-acceptance.

3 Anticipated Results

As noted above, only two QCD-based models are presently able to calculate spin observables for deuteron photodisintegration, and they provide much different predictions for the azimuthal asymmetry $\Sigma(s,t)$. Let us consider in more detail these predictions in the energy range of the g13 experiment.

QGSM predictions Within the QGSM, the spin dependence of the $\gamma d \to pn$ process has been evaluated in Refs. [48, 53] by assuming that the photodisintegration amplitude can be described by planar graphs with three-valence-quark exchange in t- or u-channels with any number of gluon exchanges between them. The spin structure of the matrix element $T(\gamma d \to pn)$ is written as [53]

$$\langle p_3,\lambda_p;p_4,\lambda_n|T(s,t)|p_2,\lambda_d;p_1,\lambda_\gamma\rangle = \bar{u}_{\lambda_p}(p_3)\hat{\epsilon}_{\lambda_\gamma}(p_1)\left[A(s,t)(\hat{p}_3-\hat{p}_1)+B(s,t)m\right]\hat{\epsilon}_{\lambda_d}(p_2)v_{\lambda_n}(p_4), \qquad (5)$$

where m is the nucleon mass, p_1, p_2, p_3 and p_4 are the 4-momenta of the photon, deuteron, proton and neutron, respectively, and λ_i denotes the s-channel helicity of the i-th particle. The invariant amplitudes $A(s,t)$ and $B(s,t)$ have similar Regge asymptotics [53]. In terms of the helicity amplitudes (5), the differential cross section for the reaction $\gamma d \to pn$ is

$$\frac{\mathrm{d}^2\sigma}{\mathrm{d}t\mathrm{d}\varphi}(s,t,\varphi) = \frac{1}{128\pi^2 s}\frac{1}{(p_\gamma^{cm})^2}\sum_{\lambda_d,\lambda_p,\lambda_n}\left|\langle p_3,\lambda_p;p_4,\lambda_n|T(s,t)|p_2,\lambda_d;p_1,\lambda_\gamma\rangle\right|^2, \qquad (6)$$

where $p_\gamma^{cm}=(s-M^2)/(2\sqrt{s})$ is the center-of-mass momentum of the photon while M is the mass of the deuteron.

The QGSM predictions for the azimuthal asymmetry $\Sigma(E_\gamma,\theta_{cm})$ in the energy range $1.2 \le E_\gamma \le 2.2$ GeV are presented in Fig. 4. One can see that the QGSM predicts sizable values for the asymmetry at large angles with a peak at $\theta_{cm}=90°$. The maximum value of $\Sigma(E_\gamma,\theta_{cm})$ decreases slowly with the photon energy from 70% at $E_\gamma=1.2$ GeV to 55% at $E_\gamma=2.2$ GeV. Note also the oscillations in the θ_{cm}-behavior of the QGSM predictions at high energies. In particular, to describe the asymmetry at $E_\gamma \approx 2$ GeV, one needs to use Legendre polynomials up to $6th$ order in $\cos\theta_{cm}$.

HRM predictions In the framework of the HRM, the spin structure of the $\gamma d \to pn$ process was considered in [54]. The quark interchange mechanism, in which quarks are exchanged between nucleons via exchange of a gluon, is used. The following result has been obtained for the spin-dependent $\gamma d \to pn$ amplitude:

$$\begin{aligned}\langle p_{\lambda_3},n_{\lambda_4}|T|\lambda_\gamma,\lambda_d\rangle &= \sum_\lambda \frac{f(\theta_{cm})\sqrt{m}}{3\sqrt{2(s-M^2)}}\left(\langle p_{\lambda_3},n_{\lambda_4}|T_{pn}(s,t_n)|p_{\lambda_\gamma/2},n_\lambda\rangle + \langle p_{\lambda_3},n_{\lambda_4}|T_{pn}(s,u_n)|n_{\lambda_\gamma/2},p_\lambda\rangle\right)\\ &\times\int \Psi_{NR}^{\lambda_d,\lambda_\gamma,\lambda}(p_z\approx 0,p_\perp)\frac{\mathrm{d}^2p_\perp}{(2\pi)^{1/2}}, \qquad (7)\end{aligned}$$

where $t_n=(p_4-\frac{1}{2}p_2)^2$, $u_n=(p_3-\frac{1}{2}p_2)^2$ and T_{pn} is the helicity amplitude of the pn scattering which is factored out of the integral. The factorization is justified (up to a scaling factor $f(\theta_{cm})$) due to the

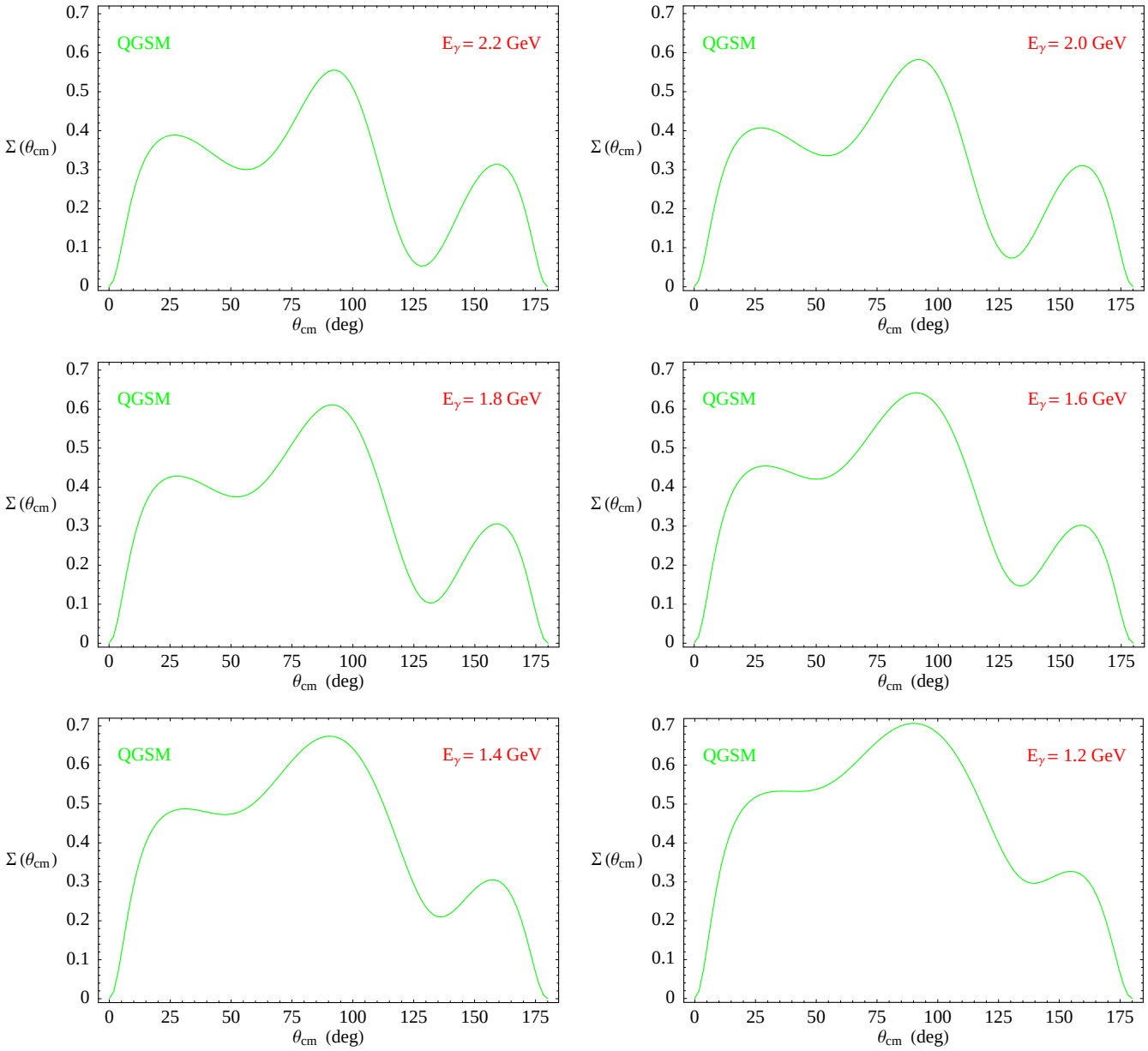

Figure 4: QGSM predictions for the azimuthal beam-spin asymmetry in deuteron photodisintegration.

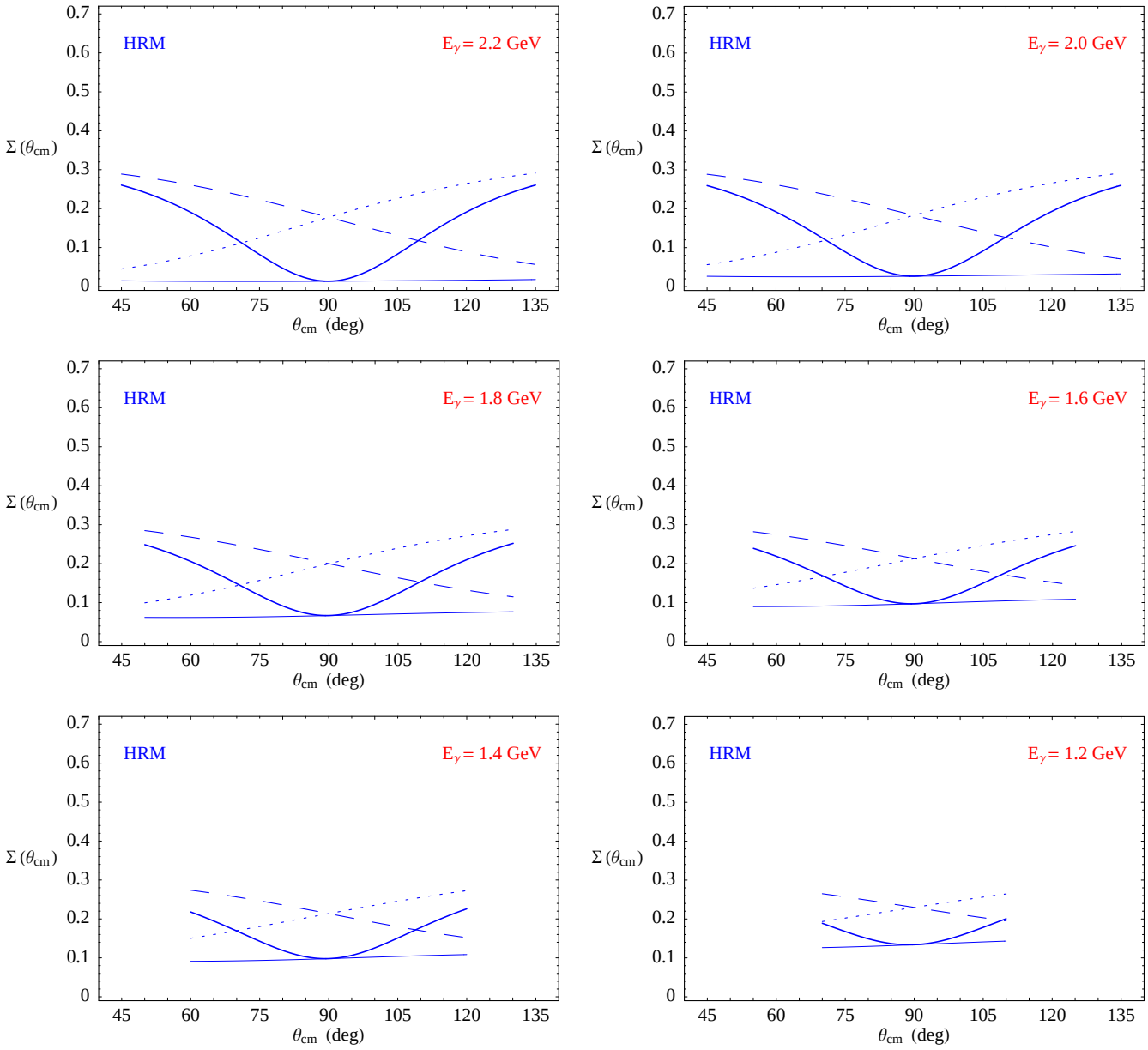

Figure 5: HRM predictions for the azimuthal beam-spin asymmetry in deuteron photodisintegration. The thick and thin solid curves correspond to the "on-shell" version of the model and represent the calculations with large and small helicity nonconservation, respectively. The dashed and dotted lines represent two versions of the "off-shell" approximation adopted in Ref. [54].

fact that the momenta involved in the integral are much smaller than the transferred momenta in the T_{pn} amplitude. For this reason, a nonrelativistic deuteron wave function $\Psi_{NR}^{\lambda_d,\lambda_\gamma,\lambda}(p)$ is used where p is the relative momentum of the nucleons in the initial state. Note that both $f(\theta_{cm})$ and $\Psi_{NR}^{\lambda_d,\lambda_\gamma,\lambda}(p)$ cancel in Eq. (3) for the asymmetry.

The results of our calculations of $\Sigma(E_\gamma, \theta_{cm})$ in the framework of the HRM are presented in Fig. 5. Since the HRM is applicable in the hard regime only ($p_T > 1$ GeV, see Ref. [45]), we do not give predictions for small angles. Note also that the condition $p_T > 1$ GeV leads to a shrinkage of the θ_{cm}-region of applicability of the model with decreasing E_γ.

Due to large uncertainties in the HRM predictions, four different lines are plotted in Fig. 5. The thick and thin solid curves correspond to the "on-shell" version of the model and represent the calculations with large and small helicity nonconservation, respectively. The dashed and dotted lines represent two versions of the "off-shell" approximation adopted in Ref. [54].

One can see from Fig. 5 that the asymmetry $\Sigma(E_\gamma, \theta_{cm})$ is predicted to be less than 30% over the entire range in energy and angle for all available versions of the HRM. We now see that the large-angle predictions of the QGSM and HRM for Σ are strongly different over the entire energy range of the g13 experiment.

4 Our Preliminary Analysis

To study in detail the feasibility of the proposed measurement, we have performed a preliminary analysis of the g13b data recorded during the 54674 and 54675 runs at the electron energy $E_e = 4.475$ GeV. Altogether forty files have been analyzed that makes up about 1% of the entire information collected in the g13 experiment for the $E_\gamma = 1.3$-1.5 GeV photon-energy bin. In the left panel of Fig. 6, we plot the photon-energy spectrum for the entire set of data gathered during the 54674 and 54675 runs.

In our preliminary analysis, only events with a single proton in final state were considered. To select the deuteron photodisintegration samples, we apply the missing-mass cuts $0.5 < M_X^2 < 1.05$ GeV^2 to the reaction $\gamma d \to pX$, where $M_X^2 = (p_\gamma + p_d - p_p)^2$. The right panel of Fig. 6 shows the photon-energy spectrum for the resulting yields. To have highly polarized photons, we use the coherent peak only, i.e. apply the cuts $1.35 < E_\gamma < 1.55$ GeV to the photon energy. As a result, we obtain about eight hundreds photodisintegration events with highly polarized photons located in the $1.35 < E_\gamma < 1.55$ GeV energy bin.

The missing-mass distributions for the reaction $\gamma d \to pX$ are presented in Fig. 7. The left panel of Fig. 7 shows the results of our Monte Carlo (MC) simulation. Altogether about 60,000 events have been generated. Solid and dashed histograms are the MC predictions for the processes $\gamma d \to pX$ and $\gamma d \to pn$, respectively. The dominant background contributions are found to be $\gamma d \to p\pi^- p$ and $\gamma d \to pn\pi^0$. They are plotted by dotted and dash-dotted lines, correspondingly. One can see from Fig. 7 that the background contribution to the number of total events under the peak is about 12%.

In the right panel of Fig. 7, a comparison of the analyzed data (full circles) with the MC predictions for the observed number of events is presented. Again, MC results for the reactions $\gamma d \to pX$ and $\gamma d \to pn$ are plotted by solid and dashed lines, correspondingly.

In our preliminary analysis, we concentrate on the scattering angles close to 90° because experimental data for Σ are available for this region only [11, 12]. Concerning the background contributions, our approach was as follows. First, we have estimated the azimuthal asymmetry at $1.2 < M_X^2 < 1.5$ GeV^2.

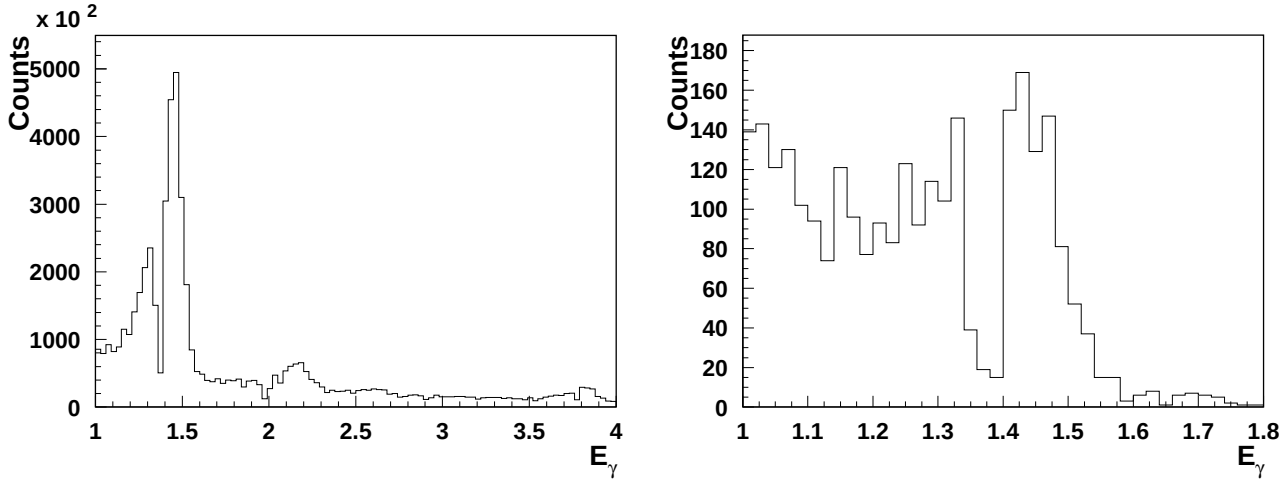

Figure 6: In the *left panel*, we plot the photon-energy spectrum for the entire set of data collected during the 54674 and 54675 runs (E_e = 4.475 GeV). The *right panel* shows the photon-energy spectrum for the deuteron photodisintegration events.

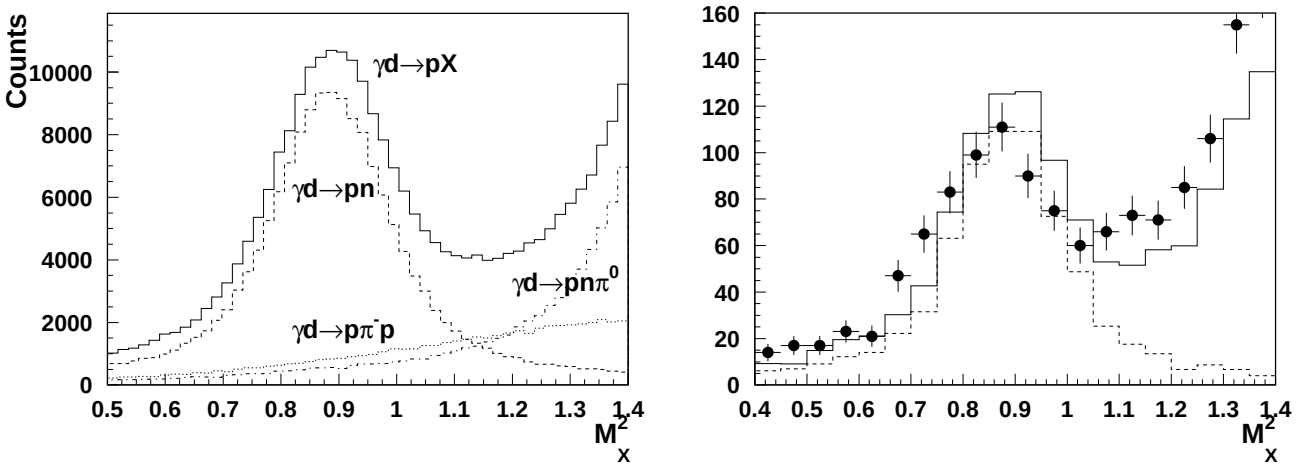

Figure 7: Missing mass distributions. The *left panel* shows the results of our MC simulation for the processes $\gamma d \to pX$, $\gamma d \to pn$, $\gamma d \to p\pi^- p$, and $\gamma d \to pn\pi^0$ (solid, dashed, dotted, and dash-dotted histograms, respectively). The *right panel* represents a comparison of the data (full circles) with the MC predictions for the available number of events.

One can see from Fig. 7 that the background channels are expected to be dominant in this region. It was found that the asymmetry is small in this domain (it is compatible with zero within the statistical errors). Then we assume that the same situation with the background asymmetry takes also place under the neutron peak. This implies that the background just dilutes the asymmetry from the deuteron photodisintegration process. In this case, one should only subtract the background from the sum $N_{\|} + N_{\perp}$ in Eq. (3) because any φ-independent contribution cancels out in the difference $N_{\|} - N_{\perp}$ by itself.

The described procedure seems to be sufficient for our preliminary analysis of data with very low statistics and relatively small background. Of course, in the final analysis of entire set of data (especially, in the high-energy region where the background is expected to be large), a more detailed, accurate account of the asymmetries in accompanying processes will be performed.

Returning to the photodisintegration process, $0.5 < M_X^2 < 1.05$ GeV^2, we have found about one hundred events in the angular bin $80^\circ < \theta_{cm} < 100^\circ$. To extract the azimuthal asymmetry Σ and subtract uncertainties due to incomplete azimuthal acceptance of the CLAS equipment, we make use the fact that, during the runs 54674 and 54675, the photon beam polarization directions were perpendicular to each other. This implies that the azimuthal distributions of the events recorded during the 54675 and 54674 runs ($\mathrm{d}N^{(+)}/\mathrm{d}\varphi$ and $\mathrm{d}N^{(-)}/\mathrm{d}\varphi$, correspondingly) have the form

$$\frac{\mathrm{d}N^{(\pm)}}{\mathrm{d}\varphi} = \frac{N_0^{(\pm)}}{2\pi}\left[1 \pm \mathcal{P}_\gamma \Sigma \cos 2\varphi\right] A(\varphi), \tag{8}$$

where the function $A(\varphi)$ accounts for an azimuthal acceptance. Note that the quantities $N_{\|}$ and $N_{\perp}$ (which define the asymmetry Σ in Eq. (3)) can be expressed in terms of $N_0^{(\pm)}$ as follows:

$$N_{\|}^{(\pm)} = \frac{N_0^{(\pm)}}{2\pi}(1 + \mathcal{P}_\gamma \Sigma), \qquad\qquad N_{\perp}^{(\pm)} = \frac{N_0^{(\pm)}}{2\pi}(1 - \mathcal{P}_\gamma \Sigma). \tag{9}$$

Defining the quantities $L^{(\pm)}(\varphi) = (2\pi/N_0^{(\pm)})(\mathrm{d}N^{(\pm)}/\mathrm{d}\varphi)$, we consider the ratio

$$\frac{1}{\mathcal{P}_\gamma}\frac{L^{(+)}(\varphi) - L^{(-)}(\varphi)}{L^{(+)}(\varphi) + L^{(-)}(\varphi)} = \Sigma \cos 2\varphi, \tag{10}$$

which should eliminate any acceptance contribution.

Our analysis of the data under consideration with the help of the ratio (10) is given in Fig. 8. Fitting the expression $C + \Sigma \cos(2\varphi + \varphi_0)$ to the data, we find that the parameters C and φ_0 are compatible (within the experimental errors) with zero while the asymmetry might be large: $\Sigma(90^\circ) = 0.50 \pm 0.19$. Note that only statistical uncertainties are taken into account.

A comparison of the obtained result with the available experimental data and theoretical predictions is given in Fig. 9. We see that our preliminary analysis of the quantity $\Sigma(90^\circ)$ is in agreement (within the experimental errors) with available Yerevan data. As to the comparison with theoretical curves, the present statistical accuracy is too low to make up any conclusion. Remember that only 1% of the CLAS data available for the range $1.3 < E_\gamma < 1.5$ GeV is taken into account. Statistical errors, anticipated after analysis of the entire set of data, are shown in Fig. 9 by filled red triangles.

In conclusion, our preliminary analysis of the 1% of the CLAS data collected in the g13 experiment indicates that the azimuthal beam-spin asymmetry for deuteron photodisintegration can be measured with an statistical accuracy varying from 2 to 8 percent in the E_γ =1.1-2.3 GeV energy range.

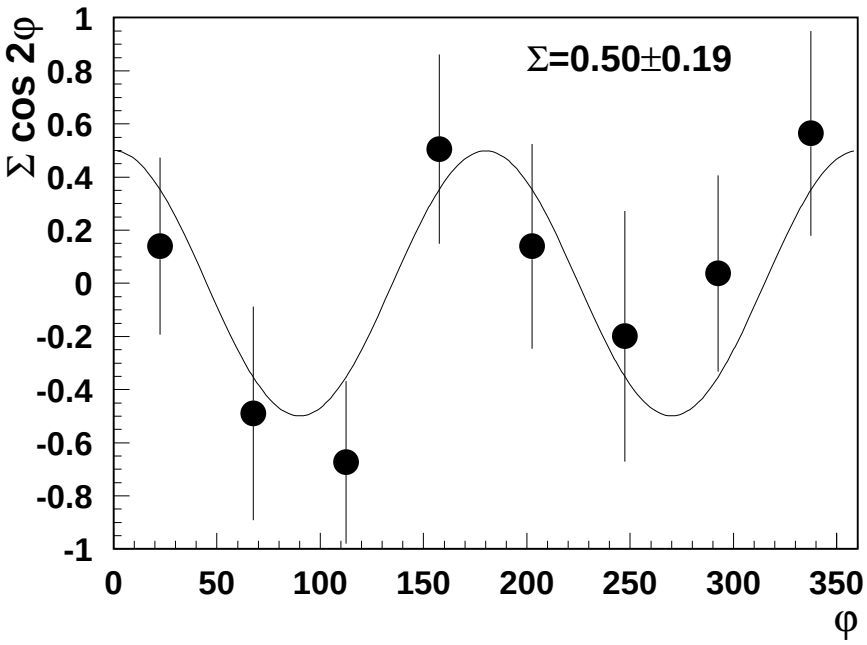

Figure 8: Our fit of the quantity $\frac{1}{\mathcal{P}_\gamma}\frac{L^{(+)}(\varphi)-L^{(-)}(\varphi)}{L^{(+)}(\varphi)+L^{(-)}(\varphi)}$ extracted from the data (see the text).

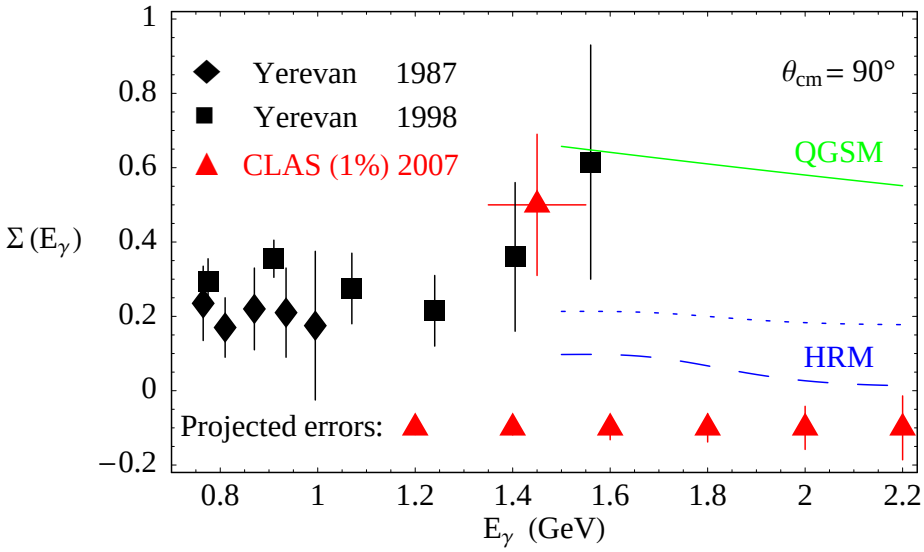

Figure 9: Comparison of our preliminary result for $\Sigma(90^\circ)$ with available experimental data and theoretical predictions.

5 Summary

We propose to determine the azimuthal beam-spin asymmetry Σ for deuteron disintegration by linearly polarized photons having energies E_γ =1.1-2.3 GeV using the CLAS data collected in g13 experiment. It is shown that the expected statistical and systematic uncertainties in the determination of the beam-spin asymmetry Σ are less than about 10%.

Our proposed analysis would

- provide new spin-dependent information on the underlying mechanism complementary to the production cross section and recoil-proton polarizations;
- improve our understanding of the role and region of applicability of perturbative QCD at low and intermediate energies;
- give access to important aspects of the long-distance dynamics, such as QCD final-state interactions and quark orbital angular momentum in the lightest nuclei; and
- provide stringent constraints on the nonperturbative QCD-based models of photonuclear reactions.

References

[1] J. Napolitano *et al.*, Phys. Rev. Lett. **61**, 2530 (1988).
[2] S. J. Freedman *et al.*, Phys. Rev. C **48**, 1864 (1993).
[3] J. E. Belz *et al.*, Phys. Rev. Lett. **74**, 646 (1995).
[4] R. Crawford *et al.*, Nucl. Phys. A **603**, 303 (1996).
[5] C. Bochna *et al.*, Phys. Rev. Lett. **81**, 4576 (1998).
[6] E. C. Schulte *et al.*, Phys. Rev. Lett. **87**, 102302 (2001).
[7] E. C. Schulte *et al.*, Phys. Rev. C **66**, 042201R (2002).
[8] M. Mirazita *et al.*, Phys. Rev. C **70**, 014005 (2004).
[9] K. Wijesooriya *et al.*, Phys. Rev. Lett. **86**, 2975 (2001).
[10] X. Jiang *et al.*, Phys. Rev. Lett. **98**, 182302 (2007).
[11] F. Adamian *et al.*, J. Phys. G **17**, 1189 (1991).
[12] F. Adamian *et al.*, Eur. Phys. J. A **8**, 423 (2000).
[13] P. Rossi *et al.*, Phys. Rev. Lett. **94**, 012301 (2005).
[14] V. Matveev, R. M. Muradyan, and A. N. Tavkhelidze, Lett. Nuovo Cimento **7**, 719 (1973).
[15] S. J. Brodsky and G. Ferrar, Phys. Rev. Lett. **31**, 1153 (1973).
[16] G.P. Lepage and S.J. Brodsky, Phys. Rev. D **22**, 2157 (1980).
[17] J. Polchinski and M.J. Strassler, Phys. Rev. Lett. **88**, 031601 (2002);
R.C. Brower and C. I. Tan, Nucl. Phys. B **662**, 393 (2003);
O. Andreev, Phys. Rev. D **67**, 046001 (2003).
[18] J. M. Maldacena, Adv. Theor. Math. Phys. **2**, 231 (1998).
[19] R. L. Anderson *et al.*, Phys. Rev. D **14**, 679 (1976).
[20] C. White *et al.*, Phys. Rev. D **49**, 58 (1994).
[21] L. Y. Zhu *et al.*, Phys. Rev. Lett. **91**, 022003 (2003);
L. Y. Zhu *et al.*, Phys Rev. C **71**, 044603 (2005).
[22] C. W. Akerlof *et al.*, Phys. Rev. **159**, 1138 (1967);
R. C. Kammerud *et al.*, Phys. Rev. D **4**, 1309 (1971);
K. A. Jenkins *et al.*, Phys. Rev. Lett. **40**, 425 (1978).
[23] A. W. Hendry, Phys. Rev. D **10**, 2300 (1974).
[24] D. P. Owen *et al.*, Phys. Rev. **181**, 1794 (1969);
K. A. Jenkins *et al.*, Phys. Rev. D **21**, 2445 (1980);
C. Baglin *et al.*, Nucl. Phys. B **216**, 1 (1983).
[25] D. G. Meekins *et al.*, Phys. Rev. C **60**, 052201 (1999).
[26] Y. Ilieva *et al.*, AIP Conf. Proc.**842**, 431 (2006).
[27] D. G. Crabb *et al.*, Phys. Rev. Lett. **41**, 1257 (1978).
[28] G. R. Court *et al.*, Phys. Rev. Lett. **57**, 507 (1986);
T. S. Bhatia *et al.*, *ibid.* **49**, 1135 (1982);
E. A. Crosbie *et al.*, Phys. Rev. D **23**, 600 (1981).
[29] S. J. Brodsky and G. F. de Teramond, Phys. Rev. Lett. **60**, 1924 (1988).
[30] S. J. Brodsky, C. E. Carlson, and H. Lipkin, Phys. Rev. D **20**, 2278 (1979).
[31] J. P. Ralston and B. Pire, Phys. Rev. Lett. **61**, 1823 (1988);
J. P. Ralston and B. Pire, Phys. Rev. Lett. **65**, 2343 (1990).

[32] A. Sen, Phys. Rev. D **28**, 860 (1983).
[33] G. R. Farrar, G. Sterman, and H. Zhang, Phys. Rev. Lett. **62**, 2229 (1989).
[34] C. E. Carlson, M. Chachkhunashvili, and F. Myhrer, Phys. Rev. D **46**, 2891 (1992).
[35] Q. Zhao and F. E. Close, Phys. Rev. Lett. **91**, 022004 (2003);
Q. Zhao and F. E. Close, Int. J. Mod. Phys. A **20**, 1910 (2005).
[36] X. Ji, J.-P. Ma, and F. Yuan, Phys. Rev. Lett. **90**, 241601 (2003).
[37] D. Dutta and H. Gao, Phys. Rev. C **71**, 032201R (2005).
[38] S.J. Brodsky and G. F. de Teramond, Phys. Lett. B **582**, 211 (2004);
S.J. Brodsky and G. F. de Teramond, arXiv:0707.3859 [hep-ph].
[39] A. V. Belitsky, X. Ji, and F. Yuan, Phys. Rev. Lett. **91**, 092003 (2003).
[40] S. J. Brodsky *et al.*, Phys. Rev. D **69**, 076001 (2004).
[41] M. K. Jones *et al.*, Phys. Rev. Lett. **84**, 1398 (2000);
O. Gayou *et al.*, Phys. Rev. Lett. **88**, 092301 (2002).
[42] R. Gilman and F. Gross, J. Phys. G **28**, R37 (2000).
[43] S. J. Brodsky and J. R. Hiller, Phys. Rev. C **28**, 475 (1983);
S. J. Brodsky and J. R. Hiller, Phys. Rev. C **30**, 412(E) (1984).
[44] S. J. Brodsky, J. R. Hiller, C.-R. Ji, and G. A. Miller, Phys. Rev. C **64**, 055204 (2001).
[45] L. L. Frankfurt, G. A. Miller, M. M. Sargsian, and M. I. Strikman, Phys. Rev. Lett. **84**, 3045 (2000);
L. L. Frankfurt, G. A. Miller, M. M. Sargsian, and M. I. Strikman, Nucl. Phys. A **663**, 349c (2000).
[46] B. Julia-Diaz and T.- S. H. Lee, Mod. Phys. Lett. A **18**, 200 (2003).
[47] L. A. Kondratyuk *et al.*, Phys. Rev. C **48**, 2491 (1993).
[48] V. Yu. Grishina *et al.*, Eur. Phys. J. A **10**, 355 (2001).
[49] A. B. Kaidalov, Z. Phys. C **12**, 63 (1982);
A. B. Kaidalov, Surv. High Energy Phys. **13**, 265 (1999).
[50] M. Arik, Phys. Rev. D **9**, 3467 (1974);
D. D. Coon *et al.*, Phys. Rev. D **18**, 1451 (1978).
[51] S. J. Brodsky, L. L. Frankfurt, R. Gilman, J. R. Hiller, G. A. Miller, E. Piasetzky, M. M. Sargsian, and M. I. Strikman, Phys. Lett. B **578**, 69 (2004).
[52] A. E. L. Dieperink and S. I. Nagorny, Phys. Lett. B **456**, 9 (1999).
[53] V. Yu. Grishina *et al.*, Eur. Phys. J. A **19**, 117 (2004).
[54] M. Sargsian, Phys. Lett. B **587**, 41 (2004).
[55] P. Nadel-Turoński *et al.*, Proposal for JLab PAC 30, PR-06-103:
"Kaon Production on the Deuteron Using Polarized Photons", (2006),
http://www.jlab.org/exp_prog/proposals/06/PR-06-103.pdf.
[56] F. J. Klein *et al.*, submitted to Nucl. Instrum. Methods **A**.
[57] E. Dumonteil, G. Niculescu, and I. Niculescu, CLAS Note 01-006 (2001).
[58] S. Morrow *et al.*, CLAS Note 01-002 (2001).
[59] For recent information concerning the *eloss* package see E. Pasyuk, CLAS Note 07-016 (2007).